LNF-79/29

B. Esposito et al. :

MULTIHADRON PRODUCTION IN $e^+e^-$ ANNIHILATION AT
(1.45 - 1.61) GeV C.M. ENERGY.

# Multihadron Production in e⁺e⁻ Annihilation at $(1.45 \div 1.61)$ GeV c.m. Energy.

B. Esposito, A. Marini, M. Pallotta, G. Piano-Mortari and F. Ronga

*Istituto Nazionale di Fisica Nucleare, Laboratori Nazionali di Frascati - Frascati, Italia*

B. Sechi-Zorn and G. T. Zorn (*)

*Department of Physics and Astronomy*
*University of Maryland - College Park, Md 20742, USA*

M. Nigro and L. Pescara

*Istituto di Fisica dell' Università - Padova*
*Istituto Nazionale di Fisica Nucleare - Sezione di Padova, Italia*

R. Bernabei, S. D'Angelo, P. Monacelli, M. Moricca, L. Paoluzi, R. Santonico and F. Sebastiani

*Istituto di Fisica dell' Università - Roma*
*Istituto Nazionale di Fisica Nucleare - Sezione di Roma, Italia*

An investigation on multihadron production in e⁺e⁻ annihilation in the centre-of-mass energy interval 1.45 to 1.61 GeV has been made at Adone, the e⁺e⁻ storage ring at Frascati, using the MEA magnetic detector. Previous preliminary results gave some indications of a resonant production at 1.5 GeV [1], but the analysis presented here does not allow us to confirm the existence of a resonant state. The results show evidence for ρ⁰ production over the whole energy range. From these data, new values for the partial cross-sections and the value of $R$ ($=$ total cross-section/$\mu\mu$ cross-section) are given.

A drawing of the MEA magnetic detector is shown in fig. 1; it is described in detail elsewhere [2]. The detector consists of wide-gap and narrow-gap spark chambers ope-

---

[1] C. Bemporad: *Proceedings of the International Symposium on Lepton and Photon Interaction at High Energies* (Hamburg, 1977).
[2] W. W. Ash, D. C. Cheng, B. Esposito, F. Felicetti, A. Marini, H. Ogren, I. Peruzzi, M. Piccolo, F. Ronga, G. Sacerdoti, L. Trasatti, G. T. Zorn, B. Bartoli, B. Coluzzi, A. Nigro, V. Silvestrini, F. Vanoli, D. Bisello, A. Mulachié, M. Nigro, L. Pescara, R. Santangelo, E. Schiavuta, D. Scannicchio, P. Monacelli, L. Paoluzi, G. Piano-Mortari and F. Sebastiani: *Nucl. Instr. and Meth.*, **148**, 431 (1978).
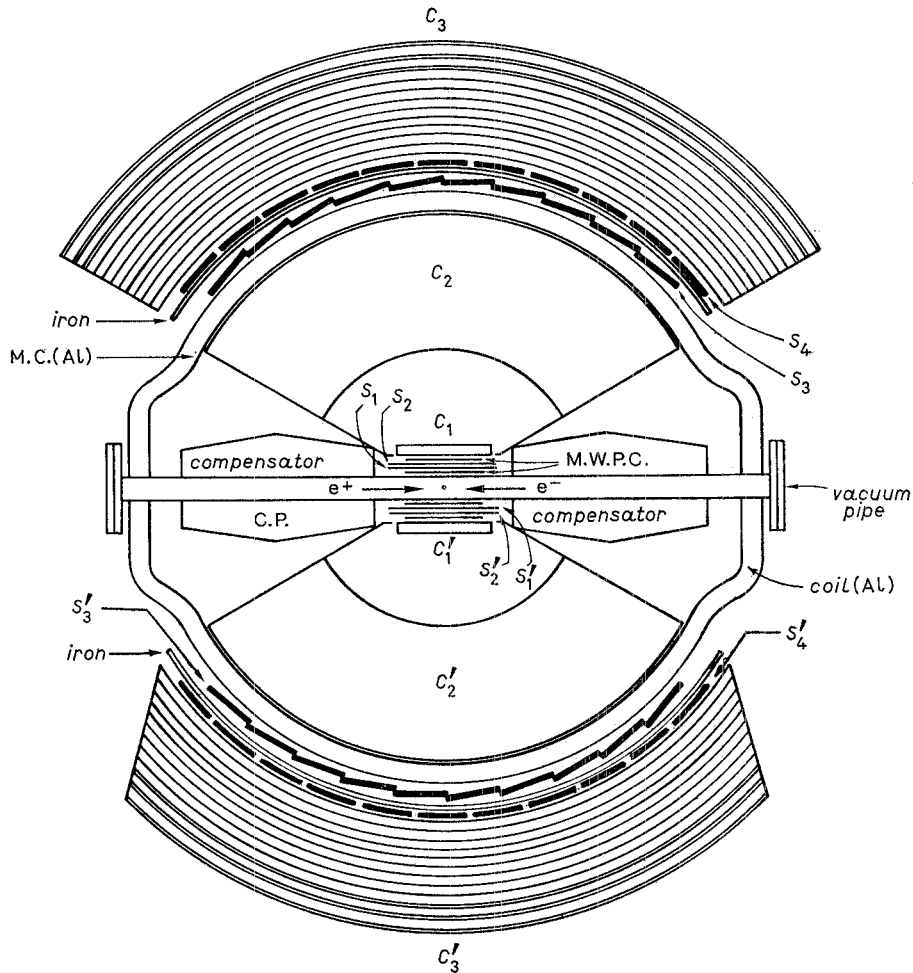
Fig. 1. – Vertical section of experimental apparatus: $C_1 C_1'$ are narrow-gap spark chamber; $C_2 C_2'$ wide-gap cylindrical spark chambers for momentum analysis; $C_3 C_3'$ thick-plate spark chambers for particle identification; MWPC multiwire proportional chambers; $S_1, S_2, ..., S_4'$ scintillation counters.

rated in a 2.0 kG magnetic field perpendicular to the $e^+e^-$ beams. The effective solid-angle acceptance for triggering and for momentum measurement at beam energies of 0.75 GeV is $\Delta\Omega_c = 0.33 \times 4\pi$ sr and for $\gamma$ conversion and for particle interaction and range studies $\Delta\Omega_N = 0.27 \times 4\pi$ sr. To trigger the apparatus two charged particles must penetrate the upper and lower halves of the detector, out to scintillation counters $S_3$ and $S_4$, thus requiring pion kinetic energies of 110 MeV and 130 MeV. The single track momentum resolution is $\Delta p/p = \pm 0.05$ at 500 MeV/c and the corresponding angular resolutions, extrapolated to the interaction region are $\Delta\varphi = \pm 1.2°$ and $\Delta\theta = \pm 0.8°$.

Photographs were scanned for multiparticle events with at least two charged tracks. The following criteria were applied in their selection: the noncolinearity angle between track pairs and the noncoplanarity angle of track pairs and the $e^+e^-$ beams were required to be $\geq 10°$; the apparent vertex point of the event should originate in the $e^+e^-$ interac-

tion region; and the event timing was required to correspond to the bunch-bunch collision time.

Studies of event timing, vertex position and secondary particle interactions have demonstrated that the multihadron events selected in this way have a negligible background contamination.

This event sample, corresponding to an integrated luminosity of 78 nb⁻¹, has been used to determine the yield of multihadron events as a function of e+e- centre-of-mass energy. These results are presented in fig. 2. Figures 2a) and b) show two groupings of the data. There is no significant indication seen of a resonant behaviour of the cross-section in this energy interval.
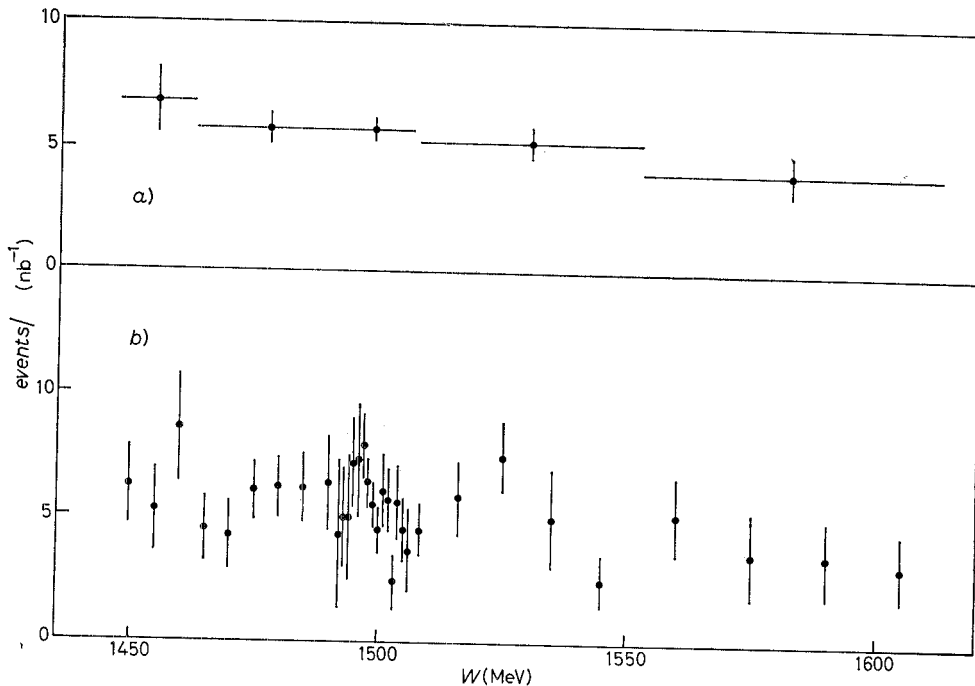


Fig. 2. – Yield of multihadron events (events/nb⁻¹) vs. e+e- centre-of-mass energy, W. a) shows individual data points and b) shows the data grouped into larger energy intervals.

From this data, a sample of events corresponding to 39 nb⁻¹ was chosen for further analysis with the objective of investigating final-state interactions and correlations. Events of at least two tracks with two wide-gap sparks defining each track were measured and reconstructed (²). The criteria for selection were the following: track-pair non colinearity and non coplanarity angles at the vertex were required to be ⩾ 10°; the tracks of an event should extrapolate to form a vertex in the interaction region within 1 cm; and, finally, the event occurrence should coincide in time with the mean bunch-bunch collision time to within ± 3 ns. A total event sample of 165 events resulted. The characteristics of these events have been summarized in table I, where the charge multiplicity is given in three centre-of-mass energy intervals.

The inclusive spectra for the selected event sample have been studied, first by comparing the spectra of the three energy intervals of table I. No statistically significant difference was noted in these inclusive spectra.

TABLE I. – *Characteristics of reconstructed events.*

| Centre-of-mass Energy, $W$ (GeV) | $L$ (nb$^{-1}$) | $2T_{Q=0}+n\gamma$ | $2T_{Q\neq0}+n\gamma$ | $3T+n\gamma$ $n=0,1,2$ | $4T+n\gamma$ | Total number of events |
|---|---|---|---|---|---|---|
| 1.450÷1.489 | 13.8 | 10 | 2 | 28 | 11 | 51 |
| 1.490÷1.510 | 16.3 | 23 | 4 | 35 | 17 | 79 |
| 1.511÷1.610 | 8.9 | 10 | 5 | 15 | 5 | 35 |
| | 39.0 | 43 | 11 | 78 | 33 | 165 |

Two-body final states coming from the decay of a known particle and resonant states, *i.e.* $K^0$, $\rho^0$ and $K^{*0}$, were investigated in an invariant mass study assuming alternately track identities of $\pi^\pm\pi^\mp$ and $K^\pm\pi^\mp$ in neutral charge combinations. Particle identities were taken consistent with time-of-flight, momentum and range measurements. Again
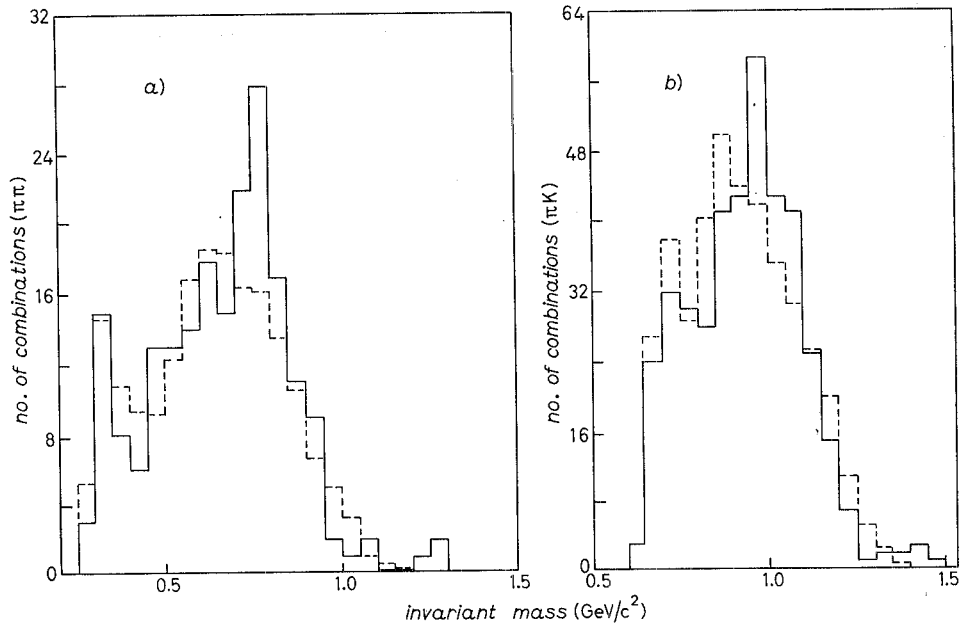


Fig. 3. – $\pi^\pm\pi^\mp$ and $\pi^\pm K^\mp$ invariant mass spectra in the energy interval $W_0 = (1.45 \div 1.61)$ GeV. Results of invariant phase space Monte Carlo calculation are shown as dashed lines.

the data were divided into 3 energy intervals as in table I to examine possible differences, Comparing these distributions no significant differences were found. These data have been combined together and the distributions of $\pi^\pm\pi^\mp$ and $\pi^\pm K^\mp$ invariant mass combinations are shown as the solid-lined histograms of fig. 3a) and b), respectively.

Also presented in fig. 3 are the results of Monte Carlo calculations in which the invariant-phase-space production of up to six pions is used (described below). The inva-

riant mass spectrum shows an enhancement at the $\rho^0$ invariant mass. The reflection of this enhancement is present in the $\pi^\pm K^\mp$ invariant mass spectrum centred at 975 MeV/c.

A search for exclusive channels was made, in particular for the channel e$^+$e$^-$ → → $\pi^+\pi^-\pi^+\pi^-$ [3-5]. In fig. 4 the spectrum of the squared missing mass $M_m^2$ is shown for the 42 events with three or four reconstructed tracks and no $\gamma$-ray (36 and 6 events respectively with $\pm 1$ and 0 total charge). Selecting the events with $-0.05 \leqslant M_m^2 \leqslant$ $\leqslant 0.15$ (GeV/c$^2$)$^2$, we obtain a set of 5 four-track and 32 three-track reconstructed events.
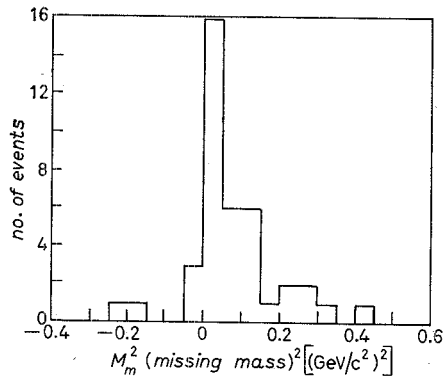


Fig. 4. – Distribution of the (missing mass)$^2$ in the energy interval $W = (1.45 \div 1.61)$ GeV for events having three or four reconstructed tracks but no converted $\gamma$-rays.

Five among the latter ones, for which the direction of the missing charged track was inside the solid angle of the apparatus, were rejected as coming from the $\pi^+\pi^-\pi^+\pi^-\pi^0$ and $\pi^+\pi^-\pi^+\pi^-\pi^0\pi^0$ channels. This number agrees with that estimated comparing the Monte Carlo calculation for these channels with the experimental $M_m^2$ distribution.

The $\pi^+\pi^-\pi^+\pi^-$ candidates were studied in a Dalitz plot of the invariant mass of a neutral pion pair vs. the mass of the other pair (fig. 5). The densities evaluated with a Monte Carlo assuming an IPS or a $\rho^0\pi^+\pi^-$ production mechanism, are shown in the upper half of the plot.

In the hypothesis of only IPS production, the comparison between experimental data and the Monte Carlo gives a $\chi^2$/d.o.f. $= 7.0$ in a fit with 4 d.o.f. The fit with IPS and $\rho^0\pi^+\pi^-$ mixed in arbitrary proportion allows us to say that the sample came essentially from the $\rho^0\pi^+\pi^-$ channel alone ($\chi^2$/d.o.f. $= 0.9$). This result is consistent with the invariant mass spectrum in fig. 3; both confirm that in this energy region the main contribution to the reaction e$^+$e$^-$ → $\pi^+\pi^-\pi^+\pi^-$ comes from the $\rho^0\pi^+\pi^-$ channel.

Assuming that only the following final-state channels contribute to the total cross-

[3]  B. Esposito, F. Felicetti, A. Marini, I. Peruzzi, M. Piccolo, F. Ronga, A. Nigro, D. Bisello, M. Nigro, L. Pescare, P. Sartori, R. Bernabei, S. d'Angelo, P. Monacelli, L. Paoluzi, G. Piano-Mortari, A. Sciubba and F. Sebastiani: Lett. Nuovo Cimento, **19**, 21 (1977).

[4]  F. Ceradini, M. Conversi, S. d'Angelo, L. Paoluzi, R. Santonico, K. Ekstrand, M. Grilli, E. Iarocci, P. Spillantini, V. Valente, R. Visentin and M. Nigro: Phys. Lett., **43** B, 341 (1973).

[5]  F. Laplanche: Proceedings of the International Symposium on Lepton and Photon Interaction at High Energies (Hamburg, 1977).
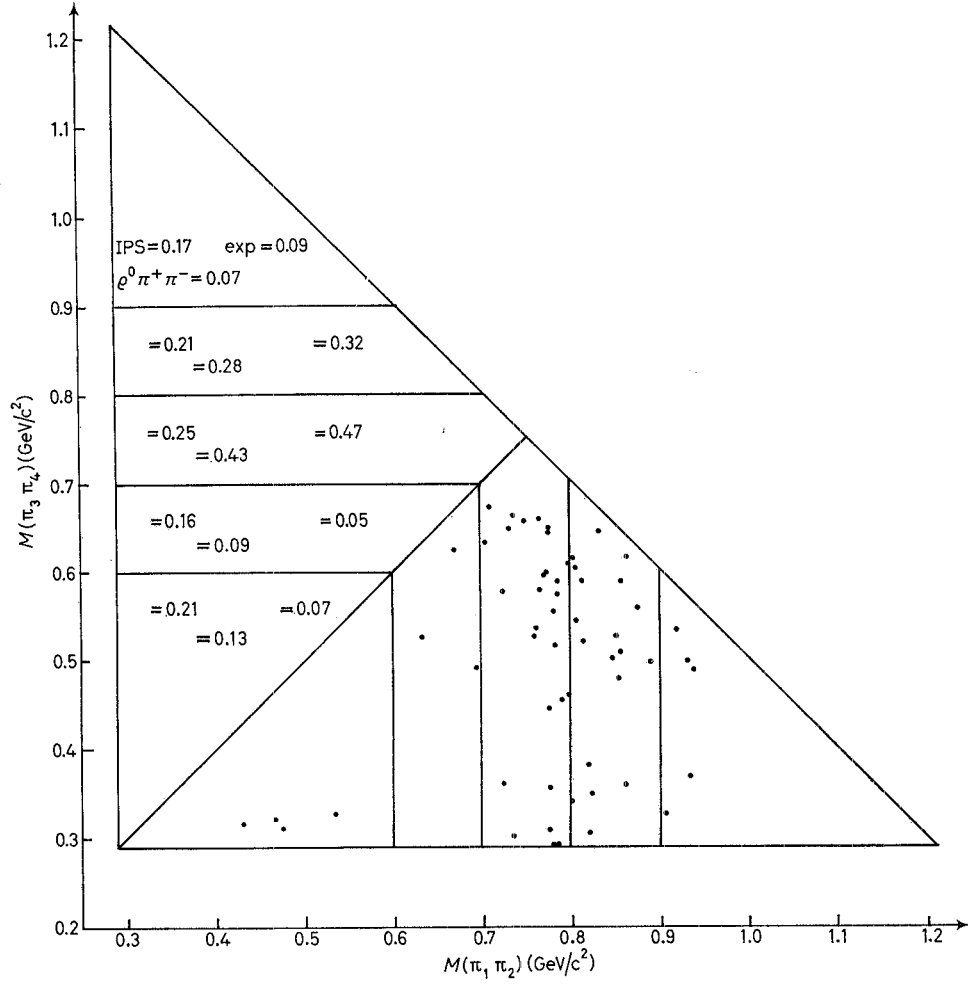
Fig. 5. – Scatter plot of the invariant mass of oppositely charged pion pairs, $M(\pi_1\pi_2)$ vs. the invariant mass of the remaining pair $M(\pi_3\pi_4)$.

section, it is possible to calculate their partial cross-sections:

$$(2) \qquad e^+e^- \rightarrow \begin{cases} \pi^+\pi^-\pi^0 \\ \pi^+\pi^-\pi^0\pi^0 \ , \\ \pi^+\pi^-\pi^0\pi^0\pi^0 \ , \\ \rho^0\pi^+\pi^- \rightarrow \pi^+\pi^-\pi^+\pi^- \ , \\ \pi^+\pi^-\pi^+\pi^-\pi^0 \ , \\ \pi^+\pi^-\pi^+\pi^-\pi^0\pi^0 \ , \\ \pi^+\pi^-\pi^+\pi^-\pi^+\pi^- \ . \end{cases}$$

TABLE II.

Efficiencies (in %) in various configurations for the detection of different final states

| $n = 0, 1, \ldots$ | $\pi^+\pi^-\pi^0$ | $\pi^+\pi^-\pi^0\pi^0$ | $\pi^+\pi^-\pi^0\pi^0\pi^0$ | $\pi^+\pi^-\pi^+\pi^-$ | $\pi^+\pi^-\pi^+\pi^-\pi^0$ | $\pi^+\pi^-\pi^+\pi^-\pi^0\pi^0$ | $\pi^+\pi^-\pi^+\pi^-\pi^+\pi^-$ | $\rho^0\pi^+\pi^-$ |
|---|---|---|---|---|---|---|---|---|
| $2T(0, n\gamma)$ | 2.20 | 2.55 | 1.20 | 4.77 | 1.98 | 0.75 | 1.13 | 4.6 |
| $2T(C, n\gamma)$ | — | — | — | 2.39 | 0.99 | 0.38 | 0.56 | 2.3 |
| $3T(n\gamma)$ | — | — | — | 5.6 | 2.58 | 1.02 | 1.70 | 6.4 |
| $4T(n\gamma)$ | — | — | — | 1.18 | 0.47 | 0.13 | 1.37 | 1.4 |
| $5T(n\gamma)$ | — | — | — | — | — | — | 0.27 | — |
| Trigger efficiencies sums (in %) | 2.20 | 2.55 | 1.20 | 13.93 | 6.02 | 2.28 | 5.06 | 14.7 |

Efficiencies (in %), for various configurations to have a squared missing mass, $M_m^2$, less than the cuts given below

| | $\pi^+\pi^-\pi^0$ | $\pi^+\pi^-\pi^0\pi^0$ | $\pi^+\pi^-\pi^0\pi^0\pi^0$ | $\pi^+\pi^-\pi^+\pi^-$ | $\pi^+\pi^-\pi^+\pi^-\pi^0$ | $\pi^+\pi^-\pi^+\pi^-\pi^0\pi^0$ | $\pi^+\pi^-\pi^+\pi^-\pi^+\pi^-$ | $\rho^0\pi^+\pi^-$ |
|---|---|---|---|---|---|---|---|---|
| $2T_R$ (a) | 100 | 0 | 0 | 0 | 0 | 0 | 0 | 0 |
| $3T_R$ | — | — | — | 100 | 39 | 0 | 0 | 100 |
| $4T_R$ | — | — | — | 100 | 0 | 0 | 0 | 100 |

(a) Where $2T_R$ are the events with: two reconstructed tracks, zero total charge, $n\gamma$ rays ($n = 0, 1, \ldots$) and $M_m^2 \leqslant 0.5$ (GeV/c²)²; $3T_R$ are the events with: three reconstructed tracks, no $\gamma$-rays and $M_m^2 \leqslant 0.15$ (GeV/c²)²; $4T_R$ are the events with: four reconstructed tracks, zero total charge, no $\gamma$-rays and $M_m^2 \leqslant 0.5$ (GeV/c²)².

In the above reactions K$^{\pm}$ production channels were not considered because of the relatively small number of K$^{\pm}$ mesons observed (*). The detection efficiencies for final states in the different detected configurations were obtained with a Monte Carlo calculation and are shown in table II. The particles were generated according to phase-space momentum distribution; only in the generation of three-body final states ($\pi^+\pi^-\pi^0$) a dynamic factor $\sin^2 \omega \sin^2 \theta$ ($^6$) was used for each event; where $\omega$ is the angle between the e$^+$e$^-$ beam direction and the normal to the production plane and $\theta$ is the angle between the two charged pions.

The partial cross-sections of the reactions (2) were evaluated solving the system of $k$ equations.

$$N_k/\mathscr{L} = \sum_i \varepsilon_{k_i} \sigma_i ,$$

where $N_k$ is the total number of events that belong to one of the categories listed in table II and that satisfy the requests on the value of their $M_m^2$ shown in the same table. $\mathscr{L}$ the total luminosity, $\sigma_i$ the cross sections for the reactions (2), $\varepsilon_{k_i}$ the efficiency for detecting the reaction $i$ in the $k$-configuration. Also the relation $\langle n_\pi \rangle = 4.2 \pm 0.1$ was used as an equation of the system to be solved, where $\langle n_\pi \rangle$ is the mean pion multiplicity obtained by the study of the inclusive spectra (**). Taking statistical errors for $N_k$ into account we have searched for the best solutions of these equations using standard programs which minimize the $\chi^2$ function.

Using the results of this analysis a complete Monte Carlo calculation was performed. From this calculation the predicted invariant mass spectra of fig. 3 were extracted. The results of this analysis are summarized in table III.

TABLE III. – Summary of calculated partial cross-sections ($\times 10^{-33}$ cm$^2$) for multihadron production at $W = (1.45 \div 1.61)$ GeV.

| | |
|---|---|
| $\sigma (\pi^+\pi^-\pi^0)$ | $2.1 \pm 2.2$ |
| $\sigma (\pi^+\pi^-\pi^0\pi^0)$ | $19.0 \pm 4.4$ |
| $\sigma (\pi^+\pi^-\pi^0\pi^0\pi^0)$ | $3.0 \pm 2.5$ |
| $\sigma (\rho^0\pi^+\pi^- \to \pi^+\pi^-\pi^+\pi^-)$ | $25.1 \pm 1.9$ |
| $\sigma (\pi^+\pi^-\pi^+\pi^-\pi^0)$ | $6.1 \pm 5.0$ |
| $\sigma (\pi^+\pi^-\pi^+\pi^-\pi^0\pi^0)$ | $15.0 \pm 5.8$ |
| $\sigma (\pi^+\pi^-\pi^+\pi^-\pi^+\pi^-)$ | $2.0 \pm 6.5$ |
| $\sigma_{tot}(e^+e^-) \to$ many-hadrons) | $72.3 \pm 11.6$ |

The total cross-section, $\sigma_{tot} = (72.3 \pm 11.6)$ nb divided by the cross-section for muon pair production is

$$R = \frac{\sigma_{tot}(e^+e^- \to \text{hadrons})}{(e^+e^- \to \mu^+\mu^-)} = 2.0 \pm 0.3 .$$

\* \* \*

We wish to thank the scanning staffs of Padova and Maryland. We are also grateful to V. BIDOLI, A. DI BIAGIO, O. CIAFFONI and S. CLEARWATER for technical assistance.

(*)   The results of this analysis will be reported in a work in progress.
($^o$)   N. CABIBBO and R. GATTO: Phys. Rev., **424**, 1577 (1961).
(**)  See note before.